

Consequences of gas flux model choice on the interpretation of metabolic balance across 15 lakes

Hilary A. Dugan, R. Iestyn Woolway, Arianto B. Santoso, Jessica R. Corman, Aline Jaimes, Emily R. Nodine, Vijay P. Patil, Jacob A. Zwart, Jennifer A. Brentrup, Amy L. Hetherington, Samantha K. Oliver, Jordan S. Read, Kirsten M. Winters, Paul C. Hanson, Emily K. Read, Luke A. Winslow & Kathleen C. Weathers

To cite this article: Hilary A. Dugan, R. Iestyn Woolway, Arianto B. Santoso, Jessica R. Corman, Aline Jaimes, Emily R. Nodine, Vijay P. Patil, Jacob A. Zwart, Jennifer A. Brentrup, Amy L. Hetherington, Samantha K. Oliver, Jordan S. Read, Kirsten M. Winters, Paul C. Hanson, Emily K. Read, Luke A. Winslow & Kathleen C. Weathers (2016) Consequences of gas flux model choice on the interpretation of metabolic balance across 15 lakes, *Inland Waters*, 6:4, 581-592, DOI: [10.1080/IW-6.4.836](https://doi.org/10.1080/IW-6.4.836)

To link to this article: <https://doi.org/10.1080/IW-6.4.836>



Published online: 02 Jan 2018.



Submit your article to this journal [↗](#)



Article views: 577



View related articles [↗](#)



View Crossmark data [↗](#)



Citing articles: 1 View citing articles [↗](#)

Consequences of gas flux model choice on the interpretation of metabolic balance across 15 lakes

Hilary A. Dugan,^{1,2,3*} R. Iestyn Woolway,⁴ Arianto B. Santoso,⁵ Jessica R. Corman,^{6,2} Aline Jaimes,⁷ Emily R. Nodine,⁸ Vijay P. Patil,⁹ Jacob A. Zwart,¹⁰ Jennifer A. Brenttrup,¹¹ Amy L. Hetherington,¹² Samantha K. Oliver,² Jordan S. Read,¹³ Kirsten M. Winters,¹⁴ Paul C. Hanson,² Emily K. Read,^{3,13} Luke A. Winslow,^{2,13} and Kathleen C. Weathers³

¹ University of Illinois at Chicago, Chicago, IL, USA

² University of Wisconsin-Madison, Madison, WI, USA

³ Cary Institute of Ecosystem Studies, Millbrook, NY, USA

⁴ Centre for Ecology & Hydrology, Lancaster, UK. Current: University of Reading, Reading, UK

⁵ University of Waikato, Hamilton, New Zealand. Current: Research Center for Limnology, Bogor, Indonesia

⁶ Arizona State University, Tempe, AZ, USA

⁷ University of Texas El Paso, El Paso, TX, USA. Current: University of Delaware, Newark, DE, USA

⁸ Florida International University, Miami, FL, USA. Current: Rollins College, Winter Park, FL, USA

⁹ University of Alaska-Fairbanks, Fairbanks, AK, USA. Current: U.S. Geological Survey, Alaska Science Center, Anchorage, AK

¹⁰ University of Notre Dame, Notre Dame, IN, USA

¹¹ Miami University, Oxford, OH, USA

¹² Cornell University, Ithaca, NY, USA. Current: Virginia Tech, Blacksburg, VA, USA.

¹³ US Geological Survey Center for Integrated Data Analytics, Middleton, WI, USA

¹⁴ Oregon State University, Corvallis, OR, USA

* Corresponding author: hilarydugan@gmail.com

Received 13 February 2015; accepted 16 February 2016; published 2 November 2016

Abstract

Ecosystem metabolism and the contribution of carbon dioxide from lakes to the atmosphere can be estimated from free-water gas measurements through the use of mass balance models, which rely on a gas transfer coefficient (k) to model gas exchange with the atmosphere. Theoretical and empirically based models of k range in complexity from wind-driven power functions to complex surface renewal models; however, model choice is rarely considered in most studies of lake metabolism. This study used high-frequency data from 15 lakes provided by the Global Lake Ecological Observatory Network (GLEON) to study how model choice of k influenced estimates of lake metabolism and gas exchange with the atmosphere. We tested 6 models of k on lakes chosen to span broad gradients in surface area and trophic states; a metabolism model was then fit to all 6 outputs of k data. We found that hourly values for k were substantially different between models and, at an annual scale, resulted in significantly different estimates of lake metabolism and gas exchange with the atmosphere.

Key words: gas exchange, GLEON, lakes, lake models, metabolism, sensor network

Introduction

Atmospheric gas exchange in lakes is routinely used to evaluate the role of lakes in global carbon cycling (Cole et al. 2007, Tranvik et al. 2009, Raymond et al. 2013). The

exchange of soluble gases, including oxygen and carbon dioxide (CO₂), across the air–water interface is influenced by physical processes such as wind stress, convection, and currents and is described by the gas transfer coefficient (k ; Zappa et al. 2007). Variability in k can span several orders

of magnitude (Wanninkhof 1992), primarily driven by diel and seasonal variations in mass and energy fluxes at the lake surface. Methods to determine k include gas tracers (Cole and Caraco 1998), floating chambers (Cole et al. 2010, Vachon et al. 2010), and eddy covariance techniques (Jonsson et al. 2008, MacIntyre et al. 2010a, Heiskanen et al. 2014). If observational data are unobtainable, k must be estimated using models.

With an estimate of k , an atmospheric flux (F) can be calculated based on dissolved oxygen (DO) concentrations and surface-mixed layer depth in a lake. This flux is often incorporated into metabolism models, which assume that changes in DO can be used as a surrogate for CO_2 based on the stoichiometric relationship between the 2 gases as part of gross primary production (GPP) and aerobic ecosystem respiration (R ; Odum 1956, Hanson et al. 2008):

$$d\text{O}_2/dt = \text{GPP} - R + F + e. \quad (1)$$

Lake metabolism is considered the net balance between GPP and R , which is equivalent to net ecosystem production (NEP; Pace and Lovett 2013) and must be balanced by F and changes in the standing stock of DO ($d\text{O}_2/dt$; equation 1). Note that an additional term (e), which accounts for the errors introduced by the inflow and outflow of oxygen, is ignored. This is an assumption applied in cases where those terms are a small part of the budget (Staehr et al. 2010).

Most approaches to estimating NEP from free-water measurements of dissolved gas assume a model for gas exchange and treat metabolism as a free parameter to be estimated (Hanson et al. 2008). Under these assumptions, any uncertainty not accounted for in k will compound error in NEP estimates. One of the most widely cited models of k is an empirically derived power function based solely on wind speed, which was developed from data collected on small lakes (Cole and Caraco 1998). Subsequently, Crusius and Wanninkhof (2003) derived a similar empirical model optimized for low wind speeds. More recently, surface renewal models have been used to incorporate the role of convective mixing on gas exchange (MacIntyre et al. 2010a, Read et al. 2012, Tedford et al. 2014). Each model has a different set of assumptions and varies in the complexity of terms and data requirements, and many models based on empirical data were developed for specific limnological and meteorological conditions. Only recently have studies begun to incorporate multiple k models (Staehr et al. 2010, Heiskanen et al. 2014, Bartosiewicz et al. 2015).

As the suite of available k models, as well as model complexity, grows, there is a need to analyze how k model choice ultimately influences NEP and gas exchange estimates (Fig. 1). Here we focus on 3 central questions: How do k values estimated from a variety of gas flux models vary, and how does this variance influence inferred NEP values? Is model choice a larger contributor to error in

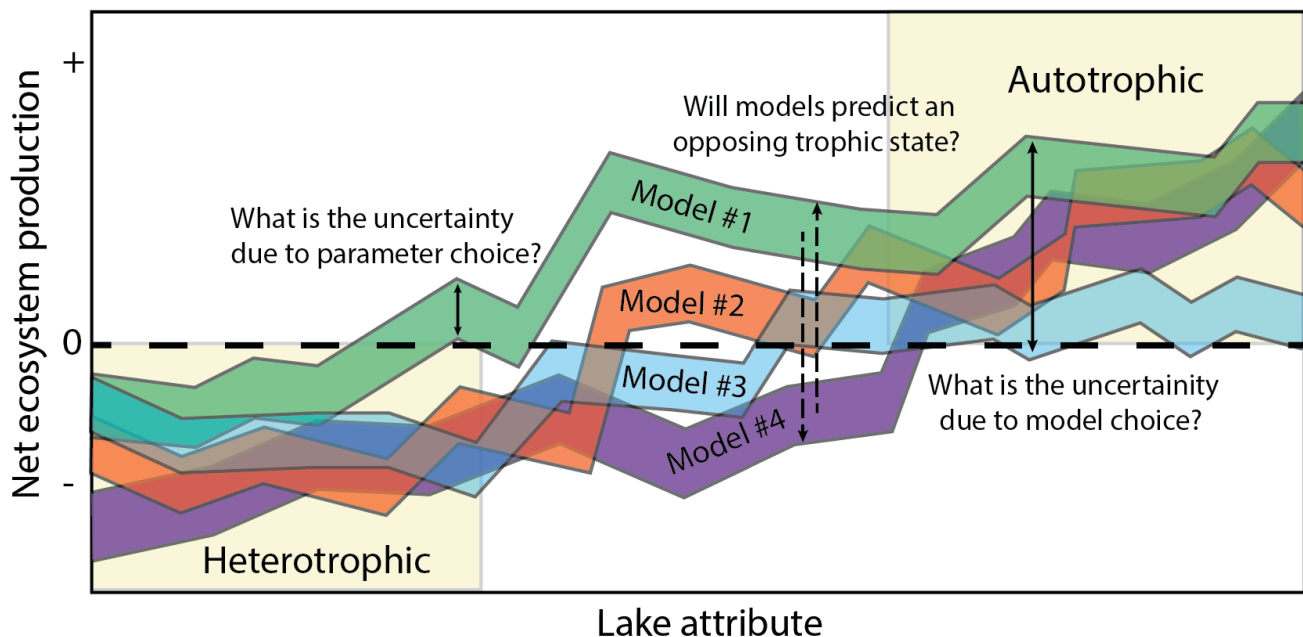


Fig. 1. Hypothetical uncertainty in net ecosystem production (NEP) estimates given a range of gas flux models. As a given lake attribute changes, each gas flux model may predict varying levels of NEP. Lake attribute could represent lake area, trophic status, or other lake characteristic.

Table 1. Physical properties of the 15 GLEON lakes included in this study. Trophic status is defined using water quality data (Carlson 1977) provided in Solomon et al. (2013) and Staehr et al. (2010). Wind height is the height at which the original wind data were recorded prior to adjustment to wind speed at 10 m height..

Lake	Lat.	Long.	Max. depth (m)	Mean depth (m)	Area (km ²)	Trophic status	Wind height (m)	Date range		Total days
Acton	39.575	−84.744	8	4	2.530	eutrophic	4.9	Apr-10	Sep-10	133
Annie	27.207	−81.351	20.7	9	0.365	mesotrophic	10	Mar-08	Feb-09	305
Castle	55.934	12.303	9	—	0.223	hyper-eutrophic	1.3	Apr-06	Nov-06	226
Crystal Bog	46.008	−89.606	2.5	2	0.005	dystrophic	2	May-08	Nov-08	149
St. Gribso	55.983	12.303	12	5	0.100	eutrophic	1.3	Apr-06	Nov-06	227
Hampensø	56.020	9.333	14	4	0.760	mesotrophic	1.3	Apr-07	Oct-07	166
Mendota	43.099	−89.652	25.3	13	39.377	eutrophic	2	Apr-09	Nov-09	213
N. Sparkling Bog	46.005	−89.705	4.3	—	0.005	dystrophic	2	Apr-09	Dec-09	228
Rotorua	−38.066	176.266	21	11	78.780	mesotrophic	1.5	Jul-07	Jul-08	338
Sparkling	46.008	−89.701	20	11	0.640	oligophic	2	May-09	Nov-09	200
Sunapee	43.383	−72.033	32	10	16.670	oligophic	2	May-08	Oct-08	148
Trout	46.029	−89.665	36	15	16.080	oligophic	2	May-08	Nov-08	155
Trout Bog	46.041	−89.686	7.9	6	0.011	dystrophic	2	May-08	Nov-08	155
Vedstedso	55.167	9.333	12	5	0.090	mesotrophic	1.3	May-08	Dec-08	202
Yuan Yang	24.583	121.402	4.5	1.7	0.036	mesotrophic	2	Jan-09	Jan-10	316

NEP estimates than the uncertainty in parameterizing GPP and R ? Under what limnological or meteorological conditions is gas flux model choice important? We capitalize on the availability of a high-frequency, multi-lake dataset associated with the Global Lake Ecological Observatory Network (GLEON, www.gleon.org) to examine the sensitivity of lake metabolism estimates to 6 published models of k across a gradient of lakes. We compare how k values differ across lakes with a range of physical and trophic states and examine which lake characteristics may influence the sensitivity of NEP and gas exchange estimates to changes in k . This comparison identifies the circumstances in which model choice is important, those in which it is not, and in what types of lakes further research is needed to establish model efficacy.

Methods

Study sites

We selected 15 temperate lakes that range in surface area from 0.005 to 79 km², in maximum depths from 2.5 to 36 m, and trophic status from oligotrophic to eutrophic (Table 1) based on the availability of high temporal frequency measurements (15–60 min sampling interval) required for estimating ecosystem metabolism (Odum 1956, Cole et al. 2000, Van de Bogert et al. 2007).

Measurements included DO, water temperature, and surface meteorology (air temperature, wind speed, relative humidity, and photosynthetically active radiation [PAR]). All data were collected between 2007 and 2010, and data for each lake include between 133 and 338 days of observation. The dataset was collected through GLEON and has been used previously in large-scale limnological analyses (Solomon et al. 2013, Rose et al. 2014). Additional information about the lakes can be found in Solomon et al. (2013).

Metabolism model

For the purpose of this investigation we used the discrete form of equation 1, similar to Solomon et al. (2013):

$$DO_{t+1} = DO_t + (\iota \times I_t) - \rho + F_t + \gamma_t \quad (2)$$

where DO_{t+1} is the concentration of DO at time $t + 1$, ι is the primary productivity per unit of PAR, I_t is the available PAR at time t , ρ is the whole-ecosystem respiration, and F_t is the flux of O_2 between the lake and the atmosphere at time t . We calculated model process error at time t as γ_t . A Nelder-Mead optimization algorithm was used to find the values of ι and ρ that minimized the negative log-likelihood of the errors, γ_t , for a given day. GPP at the daily scale was calculated from ι and the sum of PAR over the day

($GPP = \iota \times \sum I_t$). This linear relationship was chosen because more complex nonlinear equations do not generally improve metabolism estimates, especially in temperate lakes (Hanson et al. 2008). Both GPP and ρ , measured as O_2 , have units of $mg\ L^{-1}\ d^{-1}$, presented as $g\ m^{-2}\ d^{-1}$ when multiplied by the depth of the mixed layer (z_{mix}).

Gas exchange, F_t ($mg\ L^{-1}\ d^{-1}\ O_2$), was calculated as:

$$F_t = -kO_{2t} \times (DO_t - DO_{sat}) / z_{mix,t} \quad (3)$$

where DO_{sat} is the saturation concentration of O_2 ($mg\ L^{-1}$) at the current water temperature and atmospheric pressure (Benson and Krause 1984), and $z_{mix,t}$ (m) is calculated as the shallowest depth at which the rate of water density change exceeded $0.075\ kg\ m^{-3}\ m^{-1}$ (Solomon et al. 2013). The term $(DO_t - DO_{sat})$ is the deviation from saturation (DO_{diff}), where negative values indicate under-saturation of DO in the surface waters of lakes. The gas exchange coefficient for oxygen (kO_2 , $cm\ h^{-1}$) was calculated as:

$$kO_2 = k \times (ScO_2 / 600)^{-n}, \quad (4)$$

where k ($cm\ h^{-1}$) is the gas transfer coefficient, ScO_2 is the Schmidt number for O_2 calculated based on given temperature and water density (Wanninkhof 1992), and n is a dimensionless coefficient to represent the surface conditions. We followed Crusius and Wanninkhof (2003) for parameterized n values of 0.5 for wind speeds $>3\ m\ s^{-1}$ and 0.67 otherwise.

Gas transfer coefficient (k)

We calculated k from 6 published gas flux models to estimate gas exchange across all lakes (Table 2). For 5 of the published models (abbreviated as CC98, CW03, VP13, T14, and H14), we adhered to the published methods and parameters in our analysis (Cole and Caraco 1998, Crusius and Wanninkhof 2003, Vachon and Prairie 2013, Heiskanen et al. 2014, Tedford et al. 2014). Because CW03 does not describe any single model, rather 4 different models based on the same dataset, we chose the exponential form because it been used elsewhere in the literature (Staehr et al. 2012, Trolle et al. 2012). For the sixth model, we augmented the model used in Read et al. (2012) with the addition of a breaking wave component (Soloviev et al. 2007) and refer to it as R12S. All models used in this study are included in the LakeMetabolizer R package (Winslow et al. 2014, 2016).

CC98 and CW03 are univariate models based solely on wind speed, and VP13 is a bivariate model based on wind speed and lake area. Both CW03 and VP13 were developed in low-wind environments, where wind speeds did not

exceed $6\ m\ s^{-1}$ (Table 2). R12S, T14, and H14 are surface renewal models that take into account processes that generate turbulence near the air–water interface, which is quantified as the dissipation rate of turbulent kinetic energy. In T14, the mixed layer depth was set constant at 0.15 m (Bartosiewicz et al. 2015). To calculate convection, the surface energy budget was computed according to Verburg and Antenucci (2010) and buoyancy flux following Kim (1976). For all models, wind speed was normalized to a reference height of 10 m, presented as u_{10} (Schertzer et al. 2003). In certain cases, we extrapolated k models beyond the wind speeds they were developed under; however, only 2% of hourly mean wind speeds exceeded $9\ m\ s^{-1}$.

Uncertainty analysis

We were interested in understanding whether the gas flux model choice affected metabolism and gas exchange rates more or less than the uncertainty in parameterizing GPP and R (ι and ρ in equation 2) given a specific gas flux model. Within-model uncertainty, based on the parameter uncertainty of ι and ρ , was determined using a bootstrapping routine comparable to Solomon et al. (2013). To produce a distribution of metabolism estimates for each gas flux model, we determined the residual error between the optimized metabolism model and observed DO for each gas flux model. We then created pseudo-observations by selecting a random residual and constructing a time series of errors with a random normal distribution with the same autocorrelation and standard deviation and adding them to the original DO model predictions. The metabolism model was fit to the 1000 pseudo-observations to provide 1000 estimates of NEP for each day and an estimate of ι and ρ parameter uncertainty. The bootstrapped estimates were then averaged for the entire season to give 1000 mean annual NEP estimates for each lake. Values were considered significantly different between k models when 95% confidence intervals did not overlap. This bootstrapping routine provides a robust measure of within-model uncertainty. Mann-Whitney U -tests were run to test any significant differences between distributions. All modeling and analyses were performed in the R statistical package 3.0.3 (R Core Team 2014).

Representative Lakes

For illustrative purposes, we highlight data and results from 3 example lakes chosen from the dataset to represent a range in lake size and metabolism rates: Trout Bog, Acton, and Trout lakes.

- Trout Bog is a small ($0.011\ km^2$) dystrophic lake in northern Wisconsin, with a maximum depth of 7.9 m. Wind was measured at a height of 2 m, DO was

Table 2. The locations and methods used in developing each of the 6 published gas flux models. A list of data required to implement each model as well as any model constraints are provided. k_{600} is a gas transfer coefficient.

Model	Study area and methods	Results and model requirements	Reference(s)
CC98	An SF ₆ tracer experiment on Mirror Lake, NH (area 0.15 km ²) was compared with whole-system estimates from nine lakes.	Power function based on wind speed: $k_{600} = 0.215 \times u^{1.7} + 2.07$ Developed for wind speeds <9 m s ⁻¹	Cole and Caraco (1998)
CW03	An SF ₆ tracer experiment on Lake 302N (0.128 km ²) in the Experimental Lakes Area, Ontario.	Bilinear, linear and power functions based on wind speed. Power function used in this study: $k_{600} = 0.228 \times u^{10^{2.2}} + 0.168$ Developed for wind speeds <6 m s ⁻¹	Crusius and Wanninkhof (2003)
R12S	High-frequency measurements of water temperature and meteorological variables from 40 temperate lakes (0.0006–640 km ²).	k_{600} is calculated using a surface renewal model. The Read et al. (2012) model, which calculates the dissipation rate of turbulent kinetic energy as the sum of a wind shear and convection component, is augmented with a breaking wave component as in Soloviev et al. (2007). Minimum inputs: u_{10} , air temperature, relative humidity, short-wave radiation or PAR, lake area, light attenuation coefficient of PAR, depth-resolved water temperature measurements.	Read et al. (2012), Soloviev et al. (2007)
VP13	64 floating chamber measurements from a large reservoir (602 km ²) and 8 smaller temperate lakes (0.19–4.0 km ²) in Quebec.	Linear model based on wind speed and lake area (LA) was the best predictor of k_{600} . $k_{600} = 2.51 + (1.48 \times u_{10}) + (0.39 \times u_{10} \times \log_{10} LA)$ Developed for wind speeds <6 m s ⁻¹	Vachon and Prairie (2013)
T14	High-frequency water temperature and eddy covariance measurements on a temperate lake in New York, USA (4 km ²).	k_{600} is calculated using a surface renewal model, where the dissipation rate of turbulent kinetic energy is calculated separately for periods of heating and cooling. Minimum inputs: same as R12S, mixed layer depth (fixed at 0.15 m).	Tedford et al. (2014)
H14	High-frequency water temperature, dissolved CO ₂ , and eddy covariance measurements on Lake Kuivajärvi, Finland (0.63 km ²)	k_{600} is calculated using a boundary layer model that includes wind shear and cooling components. Minimum inputs: same as R12S, mixed layer depth (fixed at 0.15 m)	Heiskanen et al. (2014)

measured at 0.25 m depth, and water temperatures were measured at 0, 0.5, 1, 1.5, 2, 2.5, 3, 4, and 5 m depths.

- Acton is a shallow medium-sized (2.530 km²) eutrophic lake in southwestern Ohio, with a maximum depth of 8 m. Wind was measured at a height of 4.9 m, DO was measured at 1.5 m depth, and water temperatures were measured at 1, 3, and 5 m depths.
- Trout Lake is a large (16.080 km²) oligotrophic lake in northern Wisconsin, with a maximum depth of 36 m. Wind was measured at a height of 2 m, DO was measured at 0.5 m depth, and water temperatures were measured from 0 to 19 m at 1 m increments.

Results

In all 6 models of gas flux, k values generally increased with wind speed but showed markedly different variation and patterns among models (Fig. 2). For a given wind speed, CC98 and CW03 (univariate functions based on wind speed) returned a single k value, whereas all other models covered a range of k . When wind was negligible, CC98, CW03, and VP13 predicted k minima of 2.1, 0.2, and 2.7 cm h⁻¹, respectively. At wind speeds of 5 m s⁻¹, k ranged from 3.9 to 11.9 cm h⁻¹ across models, with the greatest variation observed in H14. At wind speeds >7 m s⁻¹, k values

were up to 20 cm h^{-1} and deviated substantially among models. Overall, T14 returned the highest k values at wind speeds $<7 \text{ m s}^{-1}$, and CC98 returned the lowest k values at wind speeds $>4 \text{ m s}^{-1}$. CW03 covered the largest range due to the extrapolation of the model to wind speeds $>6 \text{ m s}^{-1}$.

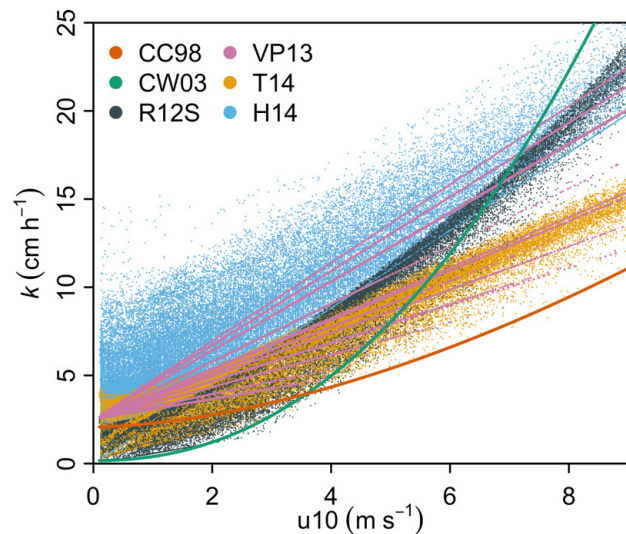


Fig. 2. Gas transfer coefficient (k) derived from 6 different models with respect to wind speeds (u_{10}) $<9 \text{ m s}^{-1}$. Data points represent hourly values for 15 GLEON lakes from a global dataset.

At diel scales, the dominant drivers of k changed across lakes and with alternative models, as illustrated in the 3 example lakes over a 3-day period in July (Fig. 3). Trout Bog is a small lake characterized by low wind speeds. Over the period of 3–6 July, daily wind speeds increased (Fig. 3a). The influence of wind speed resulted in increasing daytime k values over this period up to 6 cm h^{-1} . At night, only the surface renewal models predicted increases in k , whereas CC98, CW03, and VP13 all reached a minimum at night (Fig. 3d). Acton is larger than Trout Bog, but similar dynamics were seen in the k estimates. In both lakes, H14 returned the highest k values at night, whereas CW03 returned the lowest values overall (Fig. 3d, 3e). The third lake is Trout Lake, which is illustrative of a large waterbody. During early July, hourly wind speeds exceeded 10 m s^{-1} , and k ranged from 12 to 30 cm h^{-1} . CW03 returned k values $>30 \text{ cm h}^{-1}$, but this model was extrapolated at wind speeds $>6 \text{ m s}^{-1}$. In Trout Lake, all gas flux models predicted a similar pattern of k (Fig. 3c and f).

The density distribution of k differed in the 3 lakes (Fig. 4). CC98 and CW03 were skewed right in all lakes, with dominant peaks near 0 and 2 cm h^{-1} for CW03 and CC98, respectively. The surface renewal models were more normally distributed. Often, the peak frequency of R12S was lower than VP13, which was lower than T14 and H14 (Fig. 4).

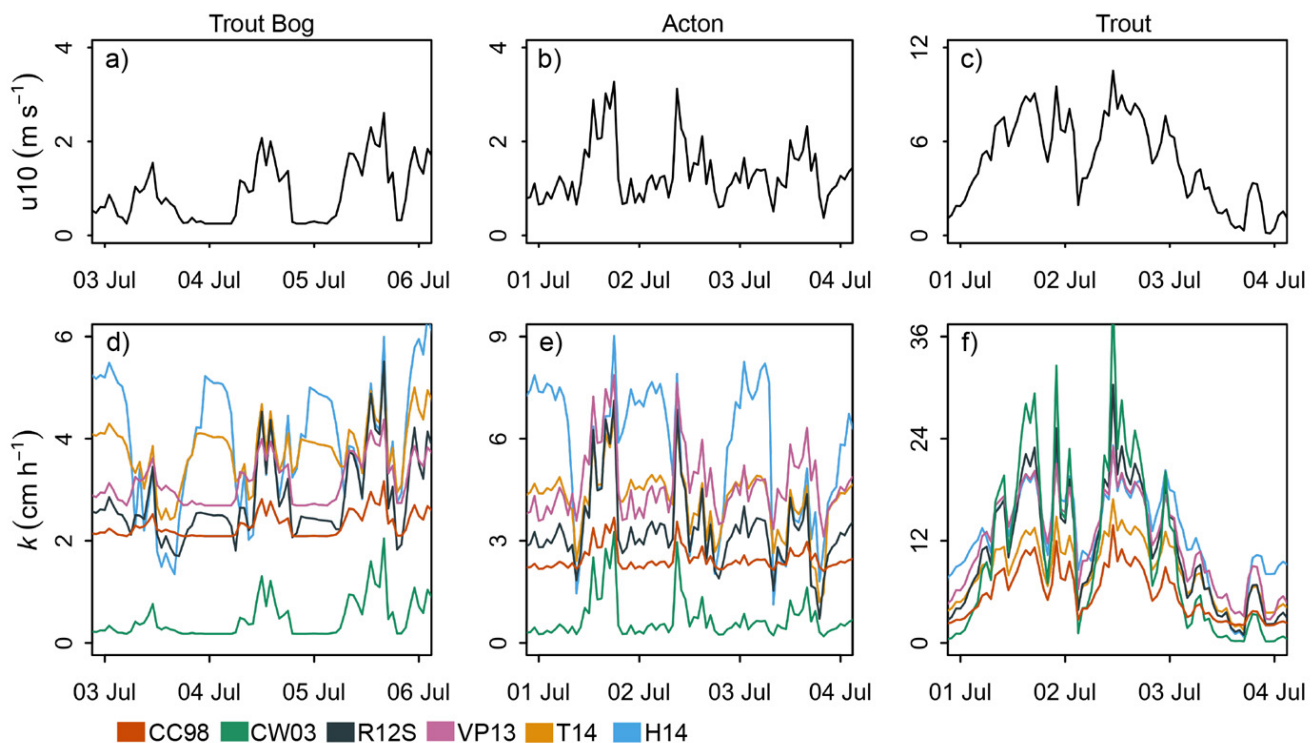


Fig. 3. (a–c) Hourly wind speed (u_{10}) for a 3-day period in early July at Trout Bog, Acton and Trout Lake. (d–f) Hourly k estimates from 6 gas flux models over the same 3-day period. Note the difference in the scale of the y-axis for all variables across the 3 lakes.

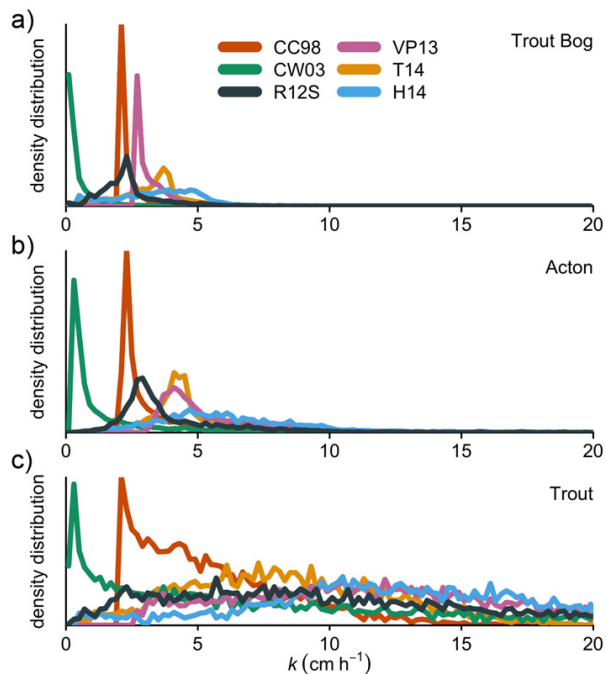


Fig. 4. Density distribution for the entire hourly record of k in Trout Bog (WI), Acton (OH) and Trout Lake (WI) for each of the 6 models.

Across the 15 lakes, there was marked variation in median wind speed, DO_{diff} , and modeled k values (Fig. 5a–c). Wind speeds and variability in wind speeds generally increased with lake size, with the exception of Annie, Acton, and Sunapee, which had lower median wind speeds than lakes of comparable size. Conversely, the range in DO_{diff} seemed unrelated to lake size. The smallest lakes (North Sparkling Bog, Crystal Bog, Trout Bog, and Yuan Yang) were all under-saturated, whereas the larger lakes showed no pattern in oxygen concentration. Of the larger lakes, the range in DO_{diff} concentrations was greatest in Castle, Acton, and Mendota and smallest in Annie, Sparkling, Trout, and Sunapee.

Overall, the gas flux models generally predicted higher k with larger lake area, which is concomitant with an increase in wind speed (Fig. 5a and c), although this correlation is biased by single-point measurements from the center of the lakes (see Schilder et al. 2013, Vachon and Prairie 2013). CW03 and CC98 generally had the lowest range of k , whereas the highest k values were from H14 in the small lakes and from VP13 and H14 in the large lakes. In larger lakes, the intra-model variability was more similar across models, and estimates showed more overlap than in small lakes.

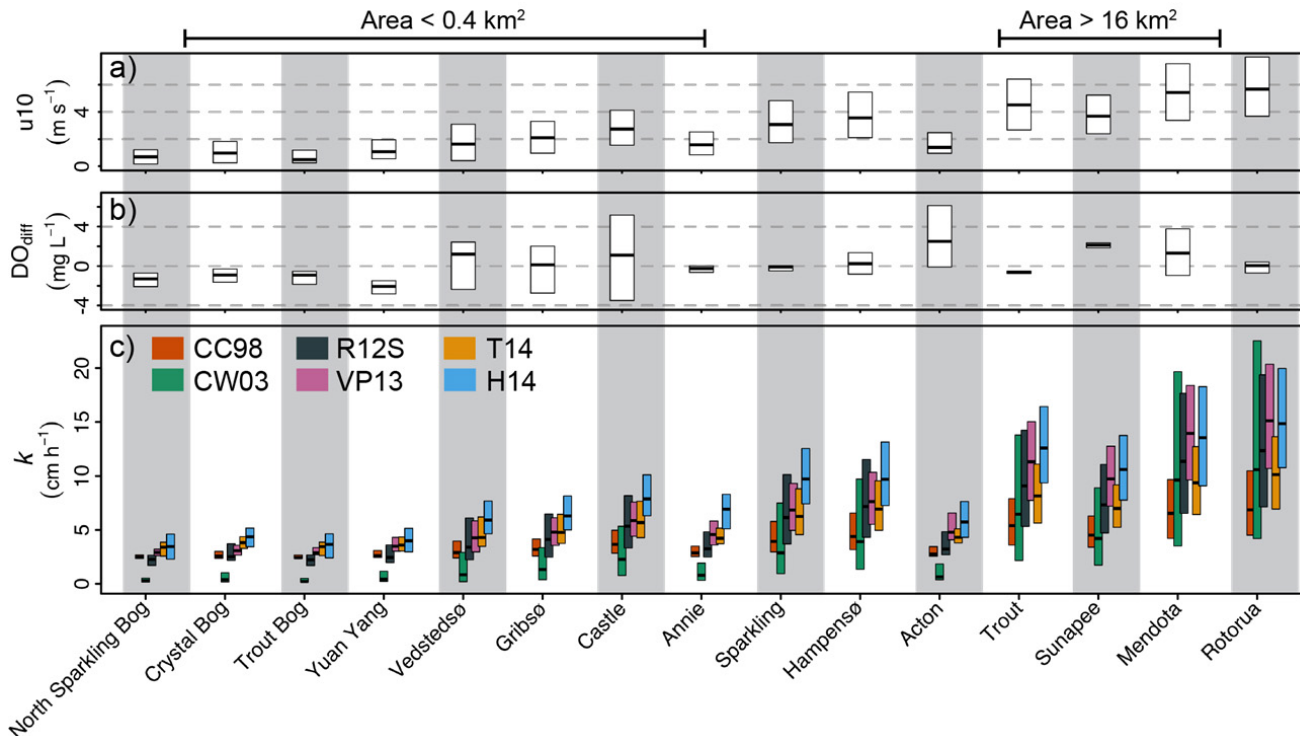


Fig. 5. Box plots of data from the full time series of (a) wind speed (u_{10}), (b) DO_{diff} , and (c) k at all 15 lakes ordered by lake area. The box edges and middle line represent the 25th, 50th (median), and 75th quartiles of the dataset.

When comparing k models in our optimized metabolism model, there was no uniform pattern in best fit; therefore, we cannot conclude that any one k model functions better across lakes. Estimated atmospheric gas exchange was highly correlated with modeled NEP, with $r^2 = 0.86$ across all models and all lakes. In the 3 example lakes, k models show broadly similar patterns in NEP through time (Fig. 6). In Trout Bog, waters became highly under-saturated in late October, and NEP estimates (measured as O_2) between models diverged beyond $-10 \text{ g m}^{-2} \text{ d}^{-1}$ (Fig. 6a). Acton, a large eutrophic lake, had positive NEP for most of the record, unless surface waters became under-saturated in DO (Fig. 6b, e, and h). Trout Lake had near saturation of DO throughout the summer, resulting in NEP close to zero and considerable model overlap (Fig. 6c, f, and i).

In all 15 lakes, mean annual NEP was significantly different between models (Mann-Whitney U -tests, $p < 0.01$, $n = 1000$). In lakes with oxygen concentrations

near equilibrium, however, NEP estimates between models were similar (Fig 7); this group of lakes includes Vestsø, Gribsø, Sparkling, Hampensø, Trout, and Rotorua. The 4 smallest lakes and large lakes Castle, Acton, Sunapee, and Mendota had a large separation in mean NEP estimates based on model choice. The 4 smallest lakes tended to be under-saturated in DO and net heterotrophic (negative NEP), whereas the larger lakes were mostly net autotrophic (positive NEP). In 8 of the lakes, H14 predicted the greatest absolute NEP values, whether for lakes with negative or positive NEP. In 3 of the largest lakes (Acton, Sunapee, and Mendota), the use of VP13 led to the highest estimated NEP. Gribsø was the only lake where model choice determined whether the estimated mean annual NEP was positive or negative. At this site, surface waters progressed from supersaturation of DO in April to under-saturation by midsummer, back to supersaturation in October.

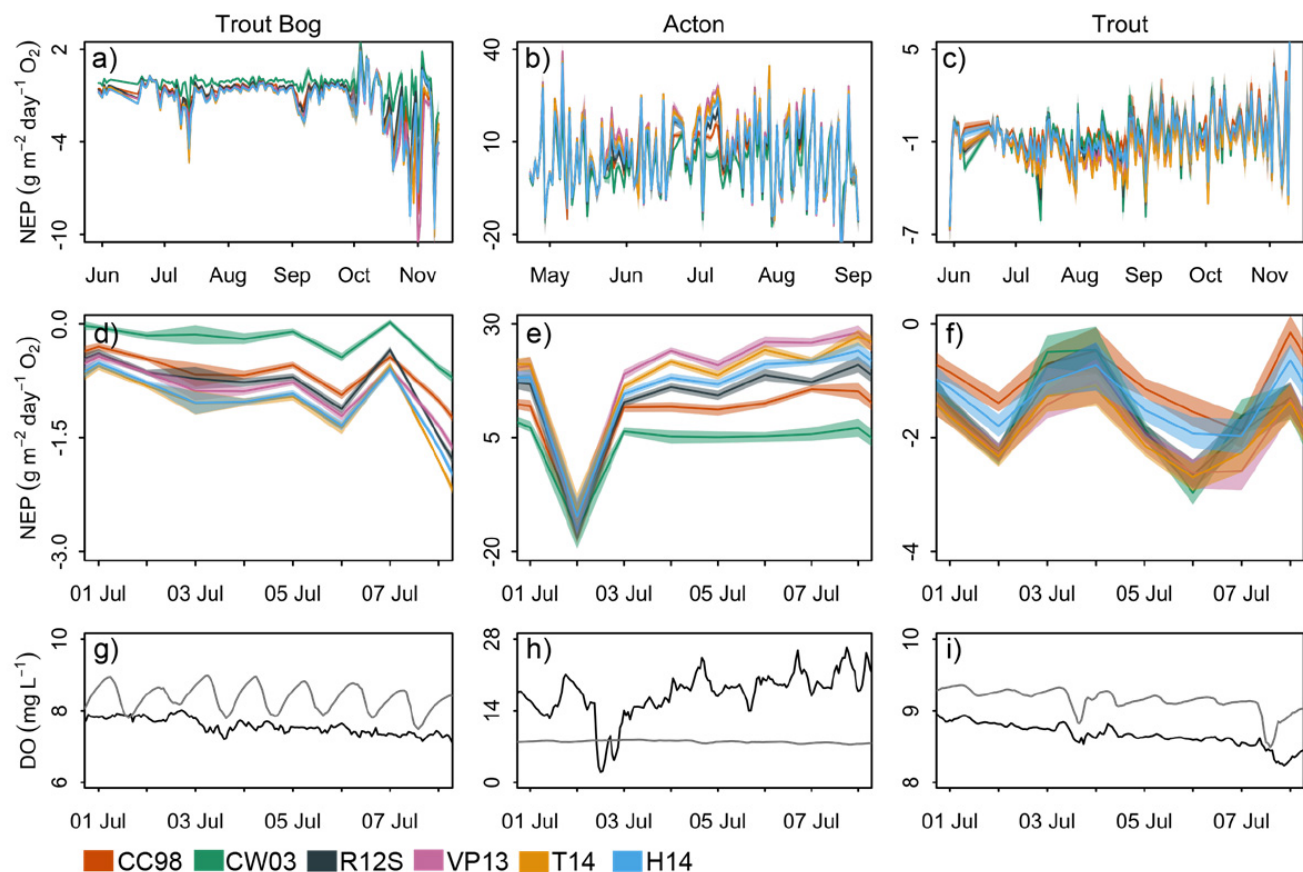


Fig. 6. (a–c) Entire record of mean daily NEP estimates at Trout Bog, Acton, and Trout lakes for the 6 models. Shaded areas around mean lines represent the 5th and 95th percentile of mean NEP estimates from the bootstrapping routine and are used to illustrate the uncertainty around ι and ρ parameter choice in the metabolism model. (d–f) Mean daily NEP estimates (measured as O_2) from 1 to 8 July for the 3 lakes. (g–i) Hourly observed dissolved oxygen concentrations (black) and concentration at saturation (gray) from 1 to 8 July. Note the difference in the scale of the y-axis for all variables across the 3 lakes.

Discussion

Our analysis demonstrates that gas flux model selection leads to a range in k values for all lakes due to the driving processes incorporated in each model. For instance, in low-wind environments, such as the bog lakes, gas exchange can be driven largely by diel heating and cooling (Read et al. 2012, Heiskanen et al. 2014, Podgrajsek et al. 2015). R12S, T14, and H14, which incorporate a convective forcing component, are potentially able to reproduce the diel variability in k caused by buoyant mixing (Fig. 3). The wind-based models have no temporal variability in low wind environments. In the 4 smallest lakes, CW03 predicted the lowest k values (Fig. 3 and 5). Because CW03 was calibrated for a lake similar in size to Gribssø, it may better represent medium sized lakes, where wind speeds are infrequently near 0 m s^{-1} and rarely $>7 \text{ m s}^{-1}$. CW03 estimates become closer to other model outputs in the larger lakes (Fig. 5).

In larger lakes, the convective aspect of the surface renewal models was less evident due to the dominance of wind-induced mixing, and these lakes exhibited a weaker diel pattern for all models (Fig. 3f). In the large lakes within our dataset ($>16 \text{ km}^2$), the high variability in k (Fig. 5) is a product of how each model treats exchange at medium to high wind speeds. For the 6 largest lakes, CC98 generally produced the lowest values of k , whereas CW03 covered the largest range. VP13 and H14 generally covered the same range of k values, whereas T14 was always slightly lower. R12S covered a range that encompassed H14 and T14 (Fig. 5). In the original R12 model (as presented in Read et al. 2012), k values became constant at high wind speeds. In our R12S model, this leveling off was compensated by the addition of a breaking wave component (Soloviev et al. 2007). In general, the large range in k estimates at wind speeds $>10 \text{ m s}^{-1}$ stems from the infrequency of high mean daily wind speeds, and therefore empirical gas flux data (Fig. 2). In our dataset, 85% of daily mean wind speeds were $<5 \text{ m s}^{-1}$ (Fig. 8).

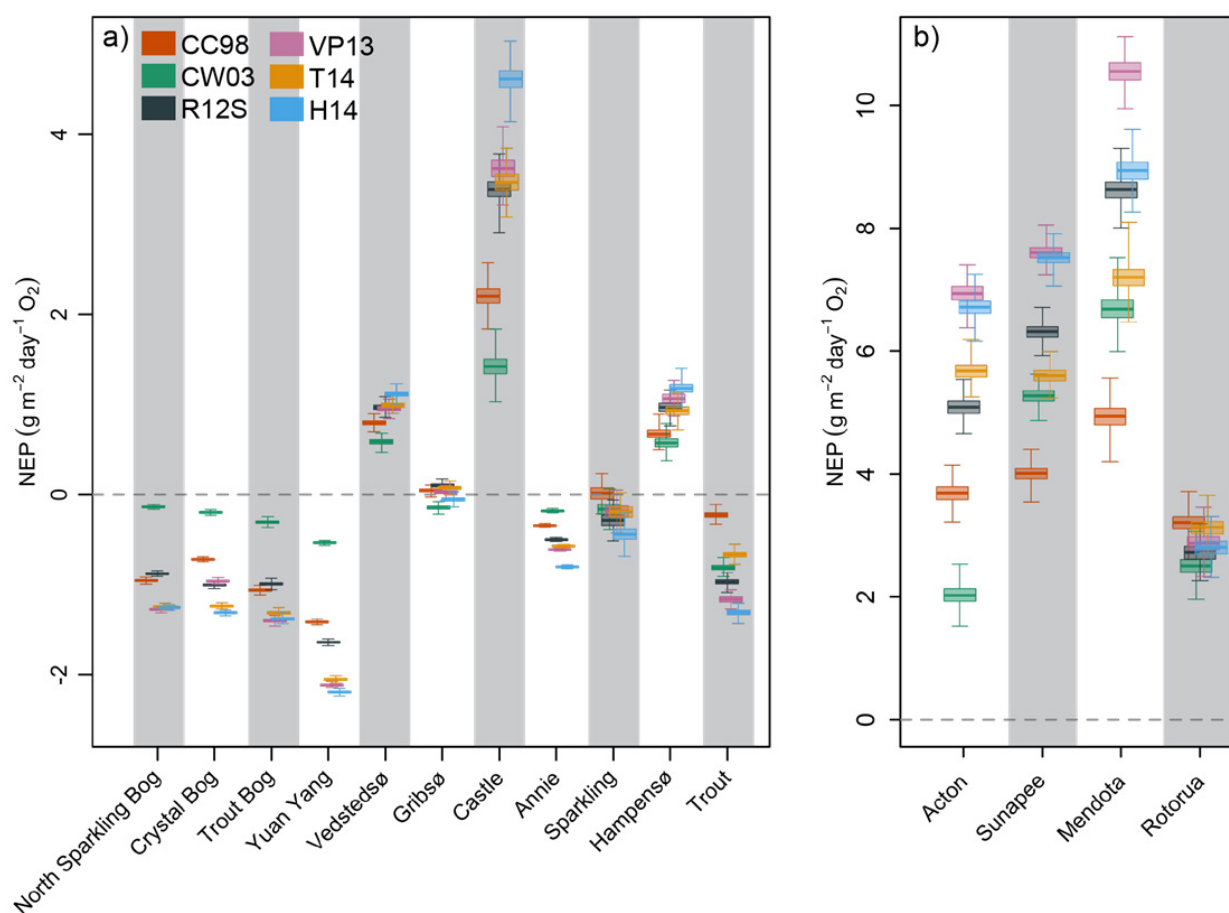


Fig. 7. Box plots of mean NEP estimates (measured as O_2) generated from the bootstrapping routine ($n = 1000$) for the full time series and for the 6 models. The plots were separated to expand the y-axis range. Lakes are ordered in ascending area, with (a) 11 smallest lakes and (b) 4 largest lakes. The exception is the order of Trout and Acton, which have been switched for legibility. Each box represents the uncertainty of the τ and ρ parameter estimates in the metabolism model. The box edges are the 25th and 75th quartiles, and the whiskers extend the full range of the data.

From our dataset of 15 lakes, we showed that gas flux model choice has a substantial effect on NEP estimates in most systems. In the small lakes, persistent under-saturation resulted in a narrow range in intra-model NEP estimates, but median NEP estimates (as O_2) varied from 0 to $-2 \text{ g m}^{-2} \text{ d}^{-1}$ (Fig. 7). In Mendota and Acton, 2 large eutrophic lakes, DO_{diff} was more variable throughout the year, and, as a result, the error in annual NEP estimates due to ι and ρ parameter uncertainty was $\sim 1 \text{ g m}^{-2} \text{ d}^{-1}$, which is much higher than seen in smaller lakes (Fig. 5). This seasonality is a critical factor in scaling-up daily estimates to annual averages and should be carefully considered when interpreting annual averages. In most lakes, the 3 surface renewal models studied here predicted larger absolute NEP than wind-based models. The exception was VP13, which compared well to H14 and R12S in most of the 15 study lakes.

Our results highlight the uncertainty in both model choice and ι and ρ parameter uncertainty but do not validate any specific model. Three important conclusions to be drawn from our results are:

1. There is more uncertainty in model choice than in the parameterization of the metabolism model.
2. NEP and DO saturation are inherently correlated, as defined in equation 3. Therefore, as surface water DO concentrations deviate from saturation, the larger the absolute range in NEP estimates will become based on any difference in k values. If DO_{diff} is known, this relationship could be considered prior to running a metabolism model.

DO_{diff} can also be incorporated lake-wide to judge spatial heterogeneity (Vachon and Prairie 2013, Schilder et al. 2013).

3. When DO concentrations fluctuate between under- and over-saturation throughout the year, model choice can govern whether the calculated mean NEP is positive or negative, as seen in Gribbsø.

Furthermore, k value outputs from VP13 closely match those from both R12S and H14. Because VP13 only requires the input of wind speed and lake area, it is easily applicable in circumstances where high-frequency meteorological and water temperature data are not available.

The eddy covariance studies cited here have argued that CC98 significantly underestimates gas flux (MacIntyre et al. 2010a, Heiskanen et al. 2014), and that k models that incorporate a buoyancy flux term better represent realistic gas flux (MacIntyre et al. 2010b, Tedford et al. 2014). Uncertainties in NEP have consequences for the interpretation of carbon budgets in lakes, and choice of k model may impact those interpretations. It may be that the traditional wind-based models have substantially underestimated the role of lakes as carbon sources and sinks. For example, CC98 has been used for large-scale lake carbon budget studies (Cardille et al. 2007, McDonald et al. 2013) and for simulating carbon balance across a broad range of load scenarios in lakes (Hanson et al. 2004). If the same studies had employed an alternative model such as H14, NEP estimates would have

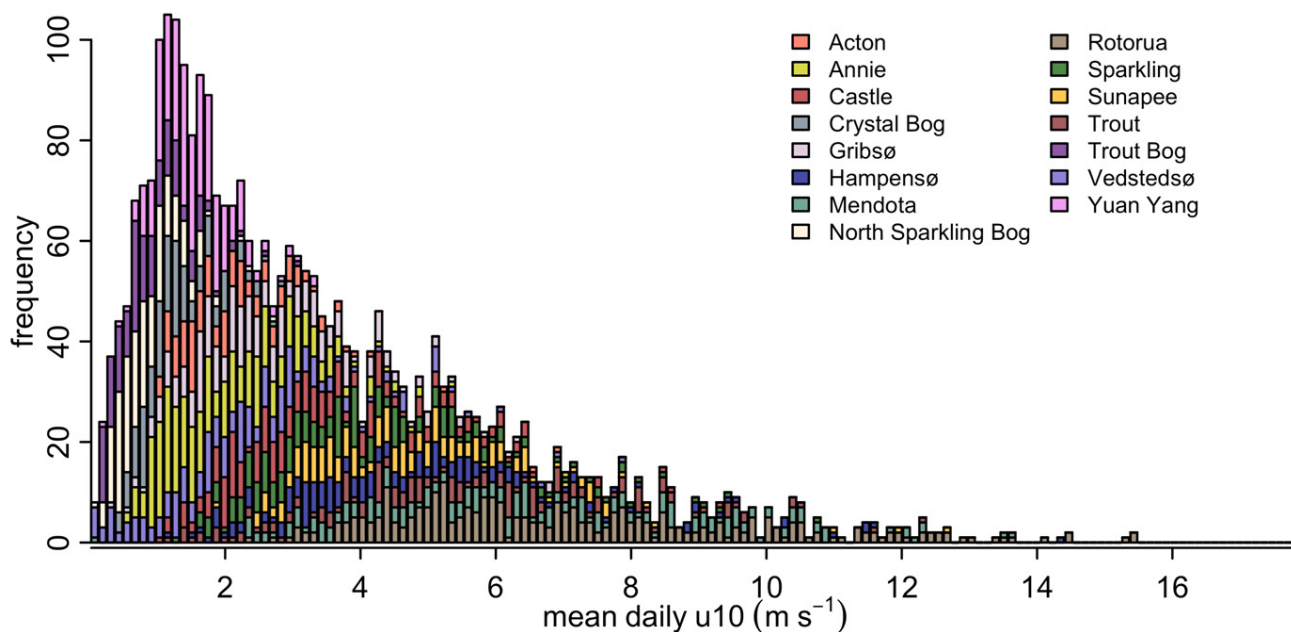


Fig. 8. Frequency distribution of mean daily wind speeds (u_{10}) stacked across the 15 lakes.

been roughly double the estimates produced using CC98 for many lakes (Fig. 7). In lakes where NEP is negative, such an increase would require a doubling of the external organic carbon load to support NEP or greatly reducing the internal production of organic carbon. In lakes where NEP is positive, the converse would be true. Either scenario would force us to rethink how we parameterize models of primary production in lakes. Similarly, in an analysis of global CO₂ emission from lakes, Raymond et al. (2013) estimated a global average gas transfer velocity by taking the average of CC98 and a highly simplified version of the R12 model. In our dataset, this would return a k value at the lower end of the range presented by all 6 gas flux models, regardless of lake size. Considering this, lakes worldwide may emit more carbon (C) than the estimated 0.3 Pg yr⁻¹ (Raymond et al. 2013).

We found that hourly values for k were substantially different between models and, at an annual scale, resulted in significantly different estimates of lake metabolism and gas exchange with the atmosphere. Ensemble modeling of gas exchange may provide a means of generalizing k in situations where the model is not calibrated to the lake. Lakes are major processing and storage sites for organic carbon (Tranvik et al. 2009, Raymond et al. 2013); thus, constraining uncertainties in NEP and determining whether lakes are net autotrophic or heterotrophic and quantifying the resulting implications regarding organic carbon loads to lakes is a high priority for future research.

Acknowledgments

This analysis is a product of the Global Lake Ecological Observatory Network (GLEON) Fellowship Program, as conceived by KCW, PCH, and EKR (<http://fellowship.gleon.org>). Open-source code for gas flux calculations can be accessed in the R package LakeMetabolizer. We do not make a distinction among the contributions of the first 8 authors in conceiving, designing, and carrying out the analysis and synthesis for this paper. All authors contributed to writing and editing of the manuscript. We thank Dr. Jonathon Cole for helpful feedback that improved this paper. Funding for this research was provided by US National Science Foundation Macrosystem Biology grant #1137353, and #1137327. Any use of trade, firm, or product names is for descriptive purposes only and does not imply endorsement by the US Government. We acknowledge data providers of the Solomon et al. (2013) dataset associated with GLEON (www.gleon.org). Data providers: Mike Vanni, Miami University (Acton Lake); Hilary Swain, Archbold Biological Station (Lake Annie); Peter Staehr, Aarhus University (Castle, St. Gribso, Hampensø, Vedstedso);

North Temperate Lakes (NTL) Long Term Ecological Research (LTER) site and the NTL Microbial Observatory (Crystal Bog, Mendota, North Sparkling Bog, Sparkling, Trout, and Trout Bog); David Hamilton, University of Waikato, New Zealand (Rotorua); Charles Chiu, Academia Sinica, Taiwan (Yuan Yang).

References

- Bartosiewicz M, Laurion I, MacIntyre S. 2015. Greenhouse gas emission and storage in a small shallow lake. *Hydrobiologia*. 757:101–115.
- Benson BB, Krause D. 1984. The concentration and isotopic fractionation of oxygen dissolved in freshwater and seawater in equilibrium with the atmosphere. *Limnol Oceanogr*. 29:620–632.
- Cardille J, Carpenter S, Coe M, Foley JA, Hanson PC, Turner MG, Vano JA. 2007. Carbon and water cycling in lake rich landscapes: landscape connections, lake hydrology, and biogeochemistry. *J Geophys Res*. 112. doi:10.1029/2006JG000200
- Carlson RE. 1977. A trophic state index for lakes. *Limnol Oceanogr*. 22:361–369.
- Cole JJ, Bade DL, Bastviken D, Pace ML, Van de Bogert MC. 2010. Multiple approaches to estimating air–water gas exchange in small lakes. *Limnol Oceanogr-Meth*. 8:285–293.
- Cole JJ, Caraco NF. 1998. Atmospheric exchange of carbon dioxide in a low-wind oligotrophic lake measured by the addition of SF₆. *Limnol Oceanogr*. 43:647–656.
- Cole JJ, Pace ML, Carpenter SR, Kitchell JF. 2000. Persistence of net heterotrophy in lakes during nutrient addition and food web manipulations. *Limnol Oceanogr*. 45:1718–1730.
- Cole JJ, Prairie Y, Caraco N. 2007. Plumbing the global carbon cycle: integrating inland waters into the terrestrial carbon budget. *Ecosystems*. 10:171–184.
- Crusius J, Wanninkhof R. 2003. Gas transfer velocities measured at low wind speed over a lake. *Limnol Oceanogr*. 48:1010–1017.
- Hanson PC, Carpenter SR, Kimura N, Wu C, Cornelius SP, Kratz TK. 2008. Evaluation of metabolism models for free-water dissolved oxygen methods in lakes. *Limnol Oceanogr-Meth*. 6:454–465.
- Hanson PC, Pollard AI, Bade DL, Predick K, Carpenter SR, Foley JA. 2004. A model of carbon evasion and sedimentation in temperate lakes. *Glob Change Biol*. 10:1285–1298.
- Heiskanen JJ, Mammarella I, Haapanala S, Pumpanen J, Vesala T, MacIntyre S, Ojala A. 2014. Effects of cooling and internal wave motions on gas transfer coefficients in a boreal lake. *Tellus B*. 66:22827.
- Jonsson A, Åberg J, Lindroth A, Jansson M. 2008. Gas transfer rate and CO₂ flux between an unproductive lake and the atmosphere in northern Sweden. *J Geophys Res*. 113:G04006.
- Kim J. 1976. A generalized bulk model of the oceanic mixed layer. *J Phys Oceanogr*. 6:686–695.
- MacIntyre S, Jonsson A, Jansson M, Åberg J, Tumey DE, Miller SD. 2010a. Buoyancy flux, turbulence, and the gas transfer coefficient in a stratified lake. *Geophys Res Lett*. 37:L24604. doi:10.1029/2010GL044164

- MacIntyre S, Jonsson A, Jansson M, Aberg J, Turney DE, Miller SD, Eugster W, Kling GW. 2010b. The critical importance of buoyancy flux for gas flux across the air-water interface. In: Donelan M, Drennan W, Saltzman E, Wanninkhof R, editors. *Gas Transf Water Surfaces*. 37.
- McDonald CP, Stets EG, Striegl RG, Butman D. 2013. Inorganic carbon loading as a primary driver of dissolved carbon dioxide concentrations in the lakes and reservoirs of the contiguous United States. *Global Biogeochem Cy*. 27:285–295.
- Odum H. 1956. Primary production in flowing waters. *Limnol Oceanogr*. 1:102–117.
- Pace ML, Lovett G. 2013. Primary production: the foundation of ecosystems. In: Weathers K, Strayer D, Likens G, editors. *Fundamentals of ecosystem science*. Academic Press. p. 312.
- Podgrajsek E, Sahlée E, Rutgersson A. 2015. Diel cycle of lake-air CO₂ flux from a shallow lake and the impact of waterside convection on the transfer velocity. *J Geophys Res Biogeosci*. doi:10.1002/2014JG002781
- R Core Team. 2014. R: a language and environment for statistical computing. Vienna, (Austria): R Foundation for Statistical Computing. Available from: <http://cran.r-project.org>
- Raymond PA, Hartmann J, Lauerwald R, Sobek S, McDonald C, Hoover M, Butman D, Striegl R, Mayorga E, Humborg C, et al. 2013. Global carbon dioxide emissions from inland waters. *Nature*. 503:355–359.
- Read JS, Hamilton DP, Desai AR, Rose KC, MacIntyre S, Lenters JD, Smyth RL, Hanson PC, Cole JJ, Staehr PA, et al. 2012. Lake-size dependency of wind shear and convection as controls on gas exchange. *Geophys Res Lett*. 39:L09405.
- Rose KC, Winslow LA, Read JS, Read EK, Solomon CT, Adrian R, Hanson PC. 2014. Improving the precision of lake ecosystem metabolism estimates by identifying predictors of model uncertainty. *Limnol Oceanogr-Meth*. 12:303–312.
- Schertzer WM, Rouse WR, Blanken PD, Walker AE. 2003. Over-lake meteorology and estimated bulk heat exchange of Great Slave Lake in 1998 and 1999. *J Hydrometeorol*. 4:649–659.
- Schilder J, Bastviken D, van Hardenbroek M, Kankaala P, Rinta P, Stötter T, Heiri O. 2013. Spatial heterogeneity and lake morphology affect diffusive greenhouse gas emission estimates of lakes. *Geophys Res Lett*. 40:5752–5756.
- Solomon C, Bruesewitz D, Richardson DC, Rose KC, Van de Bogert MC, Hanson PC, Kratz TK, Larget B, Adrian R, Babin BL, et al. 2013. Ecosystem respiration: drivers of daily variability and background respiration in lakes around the globe. *Limnol Oceanogr*. 58:849–866.
- Soloviev A, Donelan M, Graber H, Haus B, Schlüssel P. 2007. An approach to estimation of near-surface turbulence and CO₂ transfer velocity from remote sensing data. *J Mar Syst*. 66:182–194.
- Staehr PA, Bade D, Koch GR, Williamson C, Hanson P, Cole JJ, Kratz T. 2010. Lake metabolism and the diel oxygen technique: state of the science. *Limnol Oceanogr-Meth*. 8:628–644.
- Staehr PA, Testa JM, Kemp WM, Cole JJ, Sand-Jensen K, Smith SV. 2012. The metabolism of aquatic ecosystems: history, applications, and future challenges. *Aquat Sci*. 74:15–29.
- Tedford EW, MacIntyre S, Miller SD, Czikowsky MJ. 2014. Similarity scaling of turbulence in a temperate lake during fall cooling. *J Geophys Res Ocean*. 119:4689–4713.
- Tranvik L, Downing J, Cotner J, Loiselle SA, Striegl RG, Ballatore TJ, Dillon P, Finlay K, Fortino K, Knoll LB, et al. 2009. Lakes and reservoirs as regulators of carbon cycling and climate. *Limnol Oceanogr*. 54:2298–2314.
- Trolle D, Staehr PA, Davidson TA, Bjerring R, Lauridsen TL, Søndergaard M, Jeppesen E. 2012. Seasonal dynamics of CO₂ flux across the surface of shallow temperate lakes. *Ecosystems*. 15:336–347.
- Vachon D, Prairie Y, Cole JJ. 2010. The relationship between near-surface turbulence and gas transfer velocity in freshwater systems and its implications for floating chamber measurements of gas exchange. *Limnol Oceanogr*. 55:1723–1732.
- Vachon D, Prairie YT. 2013. The ecosystem size and shape dependence of gas transfer velocity versus wind speed relationships in lakes. *Can J Fish Aquat Sci*. 70:1757–1764.
- Van de Bogert MC, Carpenter SR, Cole JJ, Pace ML. 2007. Assessing pelagic and benthic metabolism using free water measurements. *Limnol Oceanogr-Meth*. 5:145–155.
- Verburg P, Antenucci JP. 2010. Persistent unstable atmospheric boundary layer enhances sensible and latent heat loss in a tropical great lake: Lake Tanganyika. *J Geophys Res*. 115:D11109.
- Wanninkhof R. 1992. Relationship between wind speed and gas exchange. *J Geophys Res*. 97:7373–7382.
- Winslow LA, Zwart J, Batt R, Corman J, Dugan HA, Hanson P, Holtgrieve G, Jaimes A, Read J, Woolway R. 2014. LakeMetabolizer: tools for the analysis of ecosystem metabolism. R Package version 1.1.
- Winslow LA, Zwart J, Batt R, Dugan H, Woolway R, Corman J, Hanson P, Read J. 2016. LakeMetabolizer: an R package for estimating lake metabolism from free-water oxygen using diverse statistical models. *Inland Waters* 6:622–636.
- Zappa CJ, McGillis WR, Raymond PA, Edson JB, Hints EJ, Zemmelen HJ, Dacey JWH, Ho DT. 2007. Environmental turbulent mixing controls on air-water gas exchange in marine and aquatic systems. *Geophys Res Lett*. 34:L10601.